Heavy hole doping of epitaxial thin films of a wide gap *p*-type semiconductor, LaCuOSe, and analysis of the effective mass

Hidenori Hiramatsu,[a] Kazushige Ueda,[b] Hiromichi Ohta,[c] and Masahiro Hirano[d]
ERATO-SORST, Japan Science and Technology Agency (JST), in Frontier Collaborative Research Center (FCRC), Tokyo Institute of Technology, S2-6F East, Mail Box S2-13, 4259 Nagatsuta-cho, Midori-ku, Yokohama 226-8503, Japan

Maiko Kikuchi, Hiroshi Yanagi, and Toshio Kamiya[e]
Materials and Structures Laboratory, Tokyo Institute of Technology, Mail Box R3-1, 4259 Nagatsuta-cho, Midori-ku, Yokohama 226-8503, Japan

Hideo Hosono[e]
Frontier Collaborative Research Center (FCRC), Tokyo Institute of Technology, S2-6F East, Mail Box S2-13, 4259 Nagatsuta-cho, Midori-ku, Yokohama 226-8503, Japan

(Received 2 May 2007; accepted 8 June 2007; published online 2 July 2007)

The high density hole doping (1.7×10^{21} cm^{-3}) for a wide gap ($E_g=\sim2.8$ eV) *p*-type semiconductor was achieved on 40 nm thick Mg-doped LaCuOSe epitaxial films. These films exhibited distinct free carrier absorption, and the effective mass and momentum relaxation time were analyzed. Its small hole mobility [~3.5 cm^2/(V s)] compared to the electron mobilities of wide gap *n*-type semiconductors is attributed to a heavy effective mass of $1.6\pm0.2m_e$. Regardless of the heavy hole doping, a band filling effect was not observed. These results are discussed with a rigid band model and an acceptor band model. © *2007 American Institute of Physics*.
[DOI: 10.1063/1.2753546]

Wide gap oxide-based semiconductors are attractive materials for short wavelength optoelectronic devices. However, *p*-type doping is more difficult than *n*-type doping for wide gap oxide-based semiconductors because the valence band maximum (VBM) of a typical oxide is formed by rather deep oxygen $2p^6$ orbitals. Oxychalcogenides, LaCuO*Ch* (*Ch*=chalcogens), which have a layered crystal structure that consists of LaO and Cu*Ch* layers and belong to the tetragonal lattice system,[1] are wide gap *p*-type semiconductors.[2] Layered oxychalcogenides have unique features such as a room temperature stable exciton,[3] *p*-type degenerate conduction,[4] and sharp photoluminescence even in a degenerate material.[5] It is noteworthy that degenerate conduction has yet to be achieved in other wide gap *p*-type semiconductors, including GaN:Mg (Refs. 6 and 7) and ZnSe:N.[8] The features of oxychalcogenides have led to the room temperature operation of blue excitonic light-emitting diodes.[9]

The key to attaining degenerate conduction was Mg^{2+} doping because Sr^{2+} and Ca^{2+} doping, which have been effective for polycrystalline samples,[2,10] were inefficient for epitaxial films. The maximum carrier concentration and electrical conductivity were less than 2.2×10^{20} cm^{-3} and 140 S cm^{-1}, respectively. However, hole injection electrode applications for current injection light-emitting devices require a higher electrical conductivity because the hole and electron injections must balance and the conductivities of wide gap *n*-type semiconductors are much higher than those of wide gap *p*-type semiconductors. In addition, although the electronic structures of LaCuO*Ch* have been investigated by photoelectron spectroscopy and *ab initio* calculations,[11–14] few experimental data associated with carrier transport properties have been obtained.

In this letter, we report that fabricating a rather thin epitaxial film enables an order of magnitude higher hole doping in Mg-doped LaCuOSe (LaCuOSe:Mg). The heavy hole doping produces a distinct free hole absorption in the near-infrared region. The effective mass and momentum relaxation time are analyzed using the transmission and reflection spectra.

LaCuOSe:Mg epitaxial thin films with different thicknesses from 40 to 150 nm were prepared on MgO (001) single-crystal substrates by reactive solid-phase epitaxy (R-SPE),[15] where a $La_{0.8}Mg_{0.2}CuOSe$ ceramic was used as the target of pulsed laser deposition and the as-deposited films were crystallized at 1000 °C with the assistance of a thin Cu sacrificial layer. Details of the growth and thermal annealing conditions are reported in Ref. 16. Chemical mechanical polishing (CMP) was employed to reduce the surface roughness of the as-prepared films. The removed thickness was less than ~10 nm. Grazing incidence x-ray reflection measurements were used to determine the film thicknesses of the as-prepared and the CMP-polished films.

Figure 1(a) shows the out-of-plane x-ray diffraction (XRD, monochromatic Cu $K\alpha_1$ radiation) pattern of a 40 nm thick LaCuOSe:Mg thin film. Only 00 *l* diffraction peaks are observed, indicating that the film is preferentially oriented along the *c* axis. The full width at half maximum of the 003 diffraction rocking curve [left inset of Fig. 1(a)] is 1.3°, demonstrating that the tilting angle of the crystallites in the LaCuOSe:Mg film is larger than that of the undoped films ($\sim0.4°$).[16] The in-plane rocking curve (ϕ scan) of the 220 diffraction [right inset of Fig. 1(a)] shows that the LaCuOSe:Mg film has a fourfold in-plane orientation, which corresponds to the tetragonal symmetry of the lattice. These observations reveal that the crystallographic orientation is (001)[110]LaCuOSe:Mg‖(001)[110]MgO.

[a]Electronic mail: h-hirama@lucid.msl.titech.ac.jp
[b]Also at Department of Materials Science, Faculty of Engineering, Kyushu Institute of Technology, Japan.
[c]Also at Graduate School of Engineering, Nagoya University, Japan.
[d]Also at FCRC, Tokyo Institute of Technology, Japan.
[e]Also at ERATO-SORST, JST, Japan.

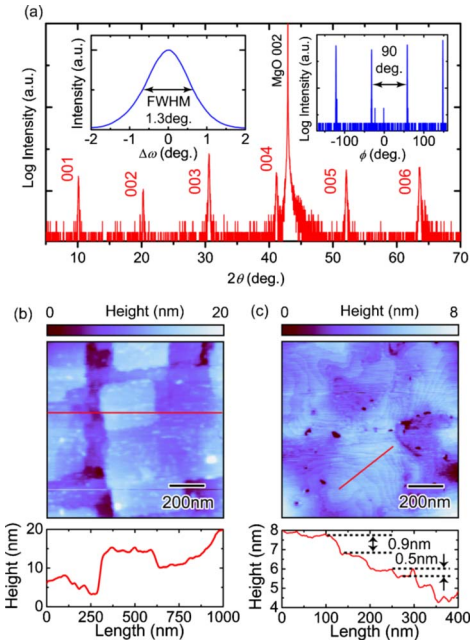

FIG. 1. (Color online) XRD patterns and AFM images of 40 nm thick LaCuOSe:Mg epitaxial films on MgO (001) single-crystal substrates. (a) Out-of-plane XRD pattern. Insets show the out-of-plane rocking curve of the 003 diffraction (left) and the in-plane ϕ scan of the 220 diffraction (right). (b) AFM image of the as-prepared film surface. (c) CMP-polished film surface. Bottom shows cross-sectional profiles along the lines in (b) and (c).

Figure 1(b) shows an atomic force microscope (AFM) image of the as-prepared LaCuOSe:Mg film with ~40 nm thickness. Tetragonal facets and very small (<30 nm) dropletlike structures with the root mean square roughness (R_{rms}) of ~3 nm are observed. This surface morphology is similar to that of previously reported thicker (~150 nm) films.[16] The observed rough surface in the thicker films was not vastly improved by polishing processes, including CMP. On the contrary, it should be noted that CMP produced an atomically flat, terrace and step surface with $R_{rms}=\sim 1$ nm for the 40 nm thick films, as shown in Fig. 1(c). The step heights are ~0.9 or ~0.5 nm, which correspond to the *c*-axis length of the unit cell and the thickness of a single molecule LaO or CuSe layer, respectively.[1]

Hall measurements using the van der Pauw configuration were performed in ac mode. Figure 2(a) shows the temperature dependence of the as-prepared and CMP-polished LaCuOSe:Mg films with 40 nm thickness. In addition, that of a 150 nm thick film in Ref. 4 is shown for comparison. Both 40 nm thick films show degenerate conduction. Moreover, surface smoothening by CMP did not change the carrier concentration and the mobility within the distribution (~10%) of the samples. Therefore, the film thickness dependence was measured using the as-prepared films [Fig. 2(b)]. Although a constant Hall mobility (μ_{Hall}) ~ 3.5 $cm^2/(V\,s)$ is maintained, the carrier concentration (n_{Hall}) gradually increases as the film thickness decreases and finally reaches $n_{Hall}=1.7\times10^{21}$ cm^{-3} and electrical conductivity $\sigma_{Hall}=910$ S cm^{-1}. These values are nearly an order of magnitude larger than those previously reported in Ref. 4 and those for other transparent *p*-type conductor films.[17] Typically, it is difficult to achieve high density hole doping for wide gap *p*-type semiconductors such as GaN:Mg,[6,7] ZnSe:N,[8] and ZnO:N (Ref. 18) due to the deep acceptor levels, which are ~100–200 meV from the VBM.

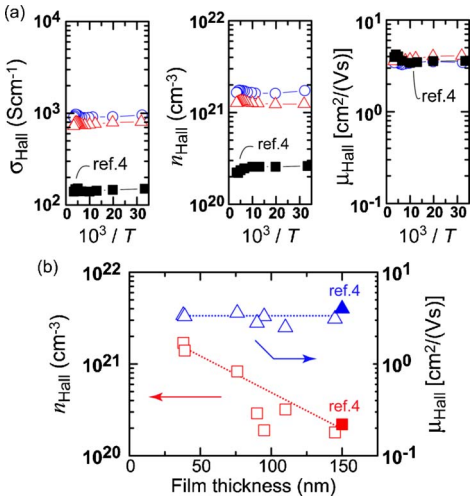

FIG. 2. (Color online) Carrier transport properties of LaCuOSe:Mg epitaxial films. σ_{Hall}, n_{Hall}, and μ_{Hall} denote the electrical conductivity, carrier concentration, and Hall mobility, respectively. (a) Temperature dependence of 40 nm thick films. Open circles and triangles show data of the as-prepared film and the CMP-polished film, respectively. (b) Variations of n_{Hall} and μ_{Hall} in the as-prepared films at room temperature with film thickness. Data previously reported for the 150 nm thick film are shown for comparison by closed symbols in (a) and (b).

Figure 3 shows the optical absorption spectrum of the Mg-doped epitaxial film. That of the undoped epitaxial film, which was fabricated by R-SPE,[16] is shown for comparison. Absorption coefficients were evaluated from transmission (T_{obs}, measured with normal incidence) and reflection spectra (R_{obs}, the incidence and reflection angles are 5° from the surface normal, respectively) using a relation $T_{net}=T_{obs}/(1-R_{obs})$ to correct the surface reflection loss. Both films have absorption peaks A and B, which originate from room temperature excitons split by a spin-orbit (SO) interaction in the Se ions.[13] Upon doping the holes at $>10^{21}$ cm^{-3}, absorption band C and absorption D appear in the visible and near-infrared regions, respectively. Band C can be understood by the defects formed by Mg^{2+} doping and/or Cu vacancies (as discussed later), while absorption D is well explained by a single Drude-type response due to free carrier absorption (FCA).[19,20] The FCA was analyzed by fitting the observed spectra to a Drude-Lorentz model where a Lorentz oscillator is employed for band C and a Drude response for absorption D. The plasma frequency (ω_p)

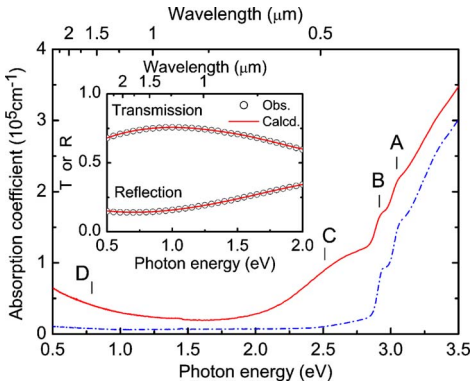

FIG. 3. (Color online) Optical absorption spectra of undoped LaCuOSe (dash-dotted line) and LaCuOSe:Mg (solid line) epitaxial films at room temperature. The inset shows the fitting result of the transmission and reflection spectra by FCA analysis. Explanation for A–D is provided in the text.

and momentum relaxation time (τ), which were determined by a least squares fitting (inset of Fig. 3), were $(1.83\pm0.08)\times10^{15}$ s^{-1} and $(4.2\pm0.5)\times10^{-15}$ s, respectively. The errors were determined by several different least squares fitting runs using different initial parameters. By assuming the carrier density value being the same as that obtained by the Hall measurement ($n_{\mathrm{Hall}}=1.7\times10^{21}$ cm^{-3}), the effective mass (m^*) value was obtained to be $1.6\pm0.2m_e$ (m_e denotes the rest mass of electron). The τ and m^* values give a FCA mobility (μ_{FCA}) of 4.6 ± 1.0 cm^2/(V s), which is slightly larger but close to $\mu_{\mathrm{Hall}}=3.4$ cm^2/(V s), verifying the validity of this analysis. The obtained τ value is comparable to those in wide gap n-type oxide semiconductors with larger mobilities [e.g., ~50 cm^2/(V s) for tin-doped In_2O_3 (ITO) (Refs. 20 and 21)] in degenerate conduction such as ITO and ZnO:Ga [$\tau=(5-7)\times10^{-15}$ s].[22] This indicates that the difference in mobility is primarily due to the difference in the m^*. A semirelativistic *ab initio* band calculation[14] reveals that the VBM is split to heavy hole (hh) and light hole (lh) bands with a SO interaction in the Se ions. The calculated m^* from the curvatures at the Γ point are $\sim0.3m_e$ for both the lh and hh bands, which do not explain the m^* ($\sim1.6m_e$) obtained by the FCA analysis. Here, it should be noticed that the LaCuOSe:Mg film is heavily doped at 1.7×10^{21} cm^{-3} and the Fermi level locates at ~0.35 eV below the VBM (estimated from the calculated total density of states and the n_{Hall}). The estimated m^* around this Fermi level are $2-3m_e$ for the hh band and $\sim1.0m_e$ for the lh band. Thus, this rigid band model semiquantitatively explains the observed m^*. However, as shown in Fig. 3, a blueshift in the optical band gap (Burstein-Moss shift[20,22]) and a change in the excitonic peak (bands A and B) positions are not observed. These observations suggest that the doped holes are mainly introduced to an acceptor band located above the VBM of pure LaCuOSe. This speculation is also consistent with the observed m^* because the corresponding bandwidth given by the simple tight binding model[19] is $2\hbar^2/m^*a^2=0.58$ eV, which is consistent with the width of band C in Fig. 3.

To clarify the origin of the thickness dependence of n_{Hall}, the depth profiles of the constituent ions were measured for the 40 and 150 nm thick films by secondary ion mass spectroscopy. Two results were obtained. The first is that the Mg concentration of the 40 nm thick film is much lower ([Mg]/[La]$<1\%$, i.e., the Mg concentration $<1.4\times10^{20}$ cm^{-3}) than that of the 150 nm thick film (~10%, $\sim1.4\times10^{21}$ cm^{-3}). Because the Mg concentration (1.4×10^{20} cm^{-3}) in the 40 nm thick film is less than 10% of the observed n_{Hall} value, the hole carriers do not originate from Mg^{2+} doping in the 40 nm thick film, although it is possible that Mg^{2+} doping generates the mobile holes in the 150 nm thick film. Another finding is that the 40 nm thick film has a depth distribution in the Cu concentration, while the 150 nm thick does not. Therefore, it is concluded that Cu vacancies are effectively formed in the thinner films to generate the high density holes. We speculate that the faster evaporation of Cu during high temperature crystallization in the R-SPE process for thinner films results in the observed thickness dependence.

In summary, high density hole doping of 1.7×10^{21} cm^{-3} for a wide gap p-type semiconductor film with an atomically flat surface is achieved. Thin (40 nm) epitaxial films of LaCuOSe:Mg show degenerate conduction with a room temperature conductivity of 910 S cm^{-1}. The hole mobility is ~3.5 cm^2/(V s), which is one order of magnitude smaller than those of n-type wide gap semiconductors, and is attributed to the heavy effective mass of $1.6\pm0.2m_e$. Two possible explanations, a rigid band model and an acceptor band model, are proposed to explain the effective mass. The wide gap p-type degenerate conduction, the high carrier concentration, and the atomically flat surface obtained by CMP make LaCuOSe:Mg a promising material for improved hole injection electrodes in optoelectronic devices such as organic and inorganic light-emitting diodes.

[1] M. Palazzi, C. R. Acad. Sci., Paris **292**, 789 (1981); W. J. Zhu, Y. Z. Huang, C. Dong, and Z. X. Zhao, Mater. Res. Bull. **29**, 143 (1994); B. A. Popovkin, A. M. Kusainova, V. A. Dolgikh, and L. G. Aksel'rud, Russ. J. Inorg. Chem. **43**, 1471 (1998); K. Takase, K. Sato, O. Shoji, Y. Takahashi, Y. Takano, K. Sekizawa, Y. Kuroiwa, and M. Goto, Appl. Phys. Lett. **90**, 161916 (2007).
[2] K. Ueda, S. Inoue, S. Hirose, H. Kawazoe, and H. Hosono, Appl. Phys. Lett. **77**, 2701 (2000).
[3] K. Ueda, S. Inoue, H. Hosono, N. Sarukura, and M. Hirano, Appl. Phys. Lett. **78**, 2333 (2001).
[4] H. Hiramatsu, K. Ueda, H. Ohta, M. Hirano, T. Kamiya, and H. Hosono, Appl. Phys. Lett. **82**, 1048 (2003).
[5] H. Hiramatsu, K. Ueda, H. Ohta, M. Hirano, T. Kamiya, and H. Hosono, Thin Solid Films **445**, 304 (2003).
[6] I. Akasaki and H. Amano, Jpn. J. Appl. Phys., Part 1 **36**, 5393 (1997).
[7] Y. Nakano and T. Jimbo, J. Appl. Phys. **92**, 5590 (2002).
[8] J. Qiu, J. M. DePuydt, H. Cheng, and M. A. Haase, Appl. Phys. Lett. **59**, 2992 (1991).
[9] H. Hiramatsu, K. Ueda, H. Ohta, T. Kamiya, M. Hirano, and H. Hosono, Appl. Phys. Lett. **87**, 211107 (2005).
[10] T. Ohtani, M. Hirose, T. Sato, K. Nagaoka, and M. Iwabe, Jpn. J. Appl. Phys., **32** (Suppl. 32-3), 316 (1993); Y. Takano, K. Yahagi, and K. Sekizawa, Physica B **206-207**, 764 (1995); K. Sekizawa, Y. Takano, K. Mori, and T. Yahagi, Czech. J. Phys. **46** (Suppl. S4), 1943 (1996); H. Hiramatsu, M. Orita, M. Hirano, K. Ueda, and H. Hosono, J. Appl. Phys. **91**, 9177 (2002).
[11] S. Inoue, K. Ueda, H. Hosono, and N. Hamada, Phys. Rev. B **64**, 245211 (2001).
[12] H. Sato, H. Negishi, A. Wada, A. Ino, S. Negishi, C. Hirai, H. Namatame, M. Taniguchi, K. Takase, Y. Takahashi, T. Shimizu, Y. Takano, and K. Sekizawa, Phys. Rev. B **68**, 035112 (2003).
[13] K. Ueda, H. Hiramatsu, H. Ohta, M. Hirano, T. Kamiya, and H. Hosono, Phys. Rev. B **69**, 155305 (2004).
[14] T. Kamiya, K. Ueda, H. Hiramatsu, H. Kamioka, H. Ohta, M. Hirano, and H. Hosono, Thin Solid Films **486**, 98 (2005).
[15] H. Ohta, K. Nomura, M. Orita, M. Hirano, K. Ueda, T. Suzuki, Y. Ikuhara, and H. Hosono, Adv. Funct. Mater. **13**, 139 (2003).
[16] H. Hiramatsu, K. Ueda, H. Ohta, M. Orita, M. Hirano, and H. Hosono, Appl. Phys. Lett. **81**, 598 (2002); H. Hiramatsu, K. Ueda, H. Ohta, M. Hirano, and H. Hosono, Mater. Res. Soc. Symp. Proc. **747**, 359 (2003); H. Hiramatsu, H. Ohta, T. Suzuki, C. Honjo, Y. Ikuhara, K. Ueda, T. Kamiya, M. Hirano, and H. Hosono, Cryst. Growth Des. **4**, 301 (2004); H. Hiramatsu, K. Ueda, K. Takafuji, H. Ohta, M. Hirano, T. Kamiya, and H. Hosono, J. Mater. Res. **19**, 2137 (2004).
[17] R. Nagarajan, A. D. Draeseke, A. W. Sleight, and J. Tate, J. Appl. Phys. **89**, 8022 (2001); H. Hiramatsu, H. Kamioka, K. Ueda, H. Ohta, T. Kamiya, M. Hirano, and H. Hosono, Phys. Status Solidi A **203**, 2800 (2006), and references therein.
[18] A. Tsukazaki, A. Ohtomo, T. Onuma, M. Ohtani, T. Makino, M. Sumiya, K. Ohtani, S. F. Chichibu, S. Fuke, Y. Segawa, H. Ohno, H. Koinuma, and M. Kawasaki, Nat. Mater. **4**, 42 (2005).
[19] P. A. Cox, *The Electronic Structure and Chemistry of Solids*, (Oxford University Press, Oxford, UK, 1987), Chap. 4.
[20] I. Hamberg and C. G. Granqvist, J. Appl. Phys. **60**, R123 (1986).
[21] H. Ohta, M. Orita, M. Hirano, H. Tanji, H. Kawazoe, and H. Hosono, Appl. Phys. Lett. **76**, 2740 (2000); H. Ohta, M. Orita, M. Hirano, and H. Hosono, J. Appl. Phys. **91**, 3547 (2002).
[22] H. Fujiwara and M. Kondo, Phys. Rev. B **71**, 075109 (2005).